Received: 7 August 2019 | Revised: 23 January 2020 | Accepted: 23 January 2020

DOI: 10.1111/gbi.12383

ORIGINAL ARTICLE

gebiology WILEY

Isotopically anomalous organic carbon in the aftermath of the Marinoan snowball Earth

Frasier L. Liljestrand[1] | Thomas A. Laakso[1] | Francis A. Macdonald[2] | Daniel P. Schrag[1] | David T. Johnston[1]

[1]Department of Earth and Planetary Sciences, Harvard University, Cambridge, MA, USA

[2]Department of Earth Sciences, University of California Santa Barbara, Santa Barbara, CA, USA

Correspondence
David T. Johnston, Department of Earth and Planetary Sciences, Harvard University, Cambridge, MA 02138, USA.
Email: johnston@eps.harvard.edu

Abstract

Throughout most of the sedimentary record, the marine carbon cycle is interpreted as being in isotopic steady state. This is most commonly inferred via isotopic reconstructions, where two export fluxes (organic carbon and carbonate) are offset by a constant isotopic fractionation of ~25 (termed $\varepsilon_{org-carb}$). Sedimentary deposits immediately overlying the Marinoan snowball Earth diamictites, however, stray from this prediction. In stratigraphic sections from the OI Formation (Mongolia) and Sheepbed Formation (Canada), we observe a temporary excursion where the organic matter has anomalously heavy $\delta^{13}C$ and is grossly decoupled from the carbonate $\delta^{13}C$. This signal may reflect the unique biogeochemical conditions that persisted in the aftermath of snowball Earth. For example, physical oceanographic modeling suggests that a strong density gradient caused the ocean to remain stratified for about 50,000 years after termination of the Marinoan snowball event, during which time the surface ocean and continental weathering consumed the large atmospheric CO_2 reservoir. Further, we now better understand how $\delta^{13}C$ records of carbonate can be post-depostionally altered and thus be misleading. In an attempt to explain the observed carbon isotope record, we developed a model that tracks the fluxes and isotopic values of carbon between the surface ocean, deep ocean, and atmosphere. By comparing the model output to the sedimentary data, stratification alone cannot generate the anomalous observed isotopic signal. Reproducing the heavy $\delta^{13}C$ in organic matter requires the progressively diminishing contribution of an additional anomalous source of organic matter. The exact source of this organic matter is unclear.

KEYWORDS

carbon cycle, carbon isotopes, organic carbon, snowball Earth

1 | INTRODUCTION

The Neoproterozoic Era (1,000–541 Ma) is a period in geologic history characterized by innovation in biology (Cohen, Strauss, Rooney, Sharma, & Tosca, 2017; Erwin et al., 2011; Knoll, 2003), the breakup of the supercontinent Rodinia (Li et al., 2008), and a series of snowball Earth events that covered the globe in ice (Hoffman, Kaufman, Halverson, & Schrag, 1998). Perturbations have been noted in the carbon, sulfur, and oxygen cycles and in certain cases are stratigraphically linked to global glaciation (Bao, Lyons, & Zhou, 2008; Hoffman et al., 1998; Hurtgen, Arthur, Suits, & Kaufman, 2002; Rothman, Hayes, & Summons, 2003). Here, much focus has

been given to the carbon cycle (cf. Halverson, Hoffman, Schrag, Maloof, & Rice, 2005; Hoffman et al., 1998), where arguments suggest a record of strong climatic and geochemical changes based on the $\delta^{13}C$ of carbonate. Although less well represented, similar studies have closed the loop providing organic carbon $\delta^{13}C$ in complement to carbonate carbon in an effort to better understand the overall biogeochemical response to these extreme climatic events (Cui, Kaufman, Xiao, Zhou, & Liu, 2017; Jiang et al., 2010; Johnston, Poulton, Tosca, O'brien, Halverson, Schrag, & Macdonald, 2013; McFadden et al., 2008; Sansjofre et al., 2011; Swanson-Hysell et al., 2010; Wang, Jiang, Shi, & Xiao, 2016). Here, we focus on the younger of the two glaciations (the Marinoan) and use the behavior of the surface carbon cycle as a vehicle to assay the nature of the biosphere and environmental change at this time.

The Marinoan snowball Earth event (>640–635 Ma) is characterized in the geologic record by evidence of glaciation at equatorial latitudes (Hoffman et al., 1998). One hypothesis is that weathering of low-latitude continents decreased atmospheric CO_2 causing a runaway glaciation (cf. Cox et al., 2016). Glaciation only terminated when volcanic emissions increased atmospheric CO_2 sufficiently for greenhouse warming to overcome the high planetary albedo that came from ice coverage (Hoffman & Schrag, 2002). The subsequently warm, high CO_2 conditions accelerated the hydrologic cycle, rapidly weathered the post-glacial continents, delivered alkalinity to the ocean, and drove global carbonate precipitation (Higgins & Schrag, 2003). In the geologic record, this is observed globally in the form of cap carbonates overlying the glacial diamictites (Hoffman et al., 1998). Synglacial carbonates are rare, so these cap carbonate deposits and the sediments above are the best window to understand both the environmental conditions adopted from a synglacial ocean and the lasting biogeochemical consequences that extended into the post-glacial world.

Recent work suggests that immediately after the Marinoan deglaciation, the ocean was intensely stratified (Yang, Jansen, Macdonald, & Abbot, 2017). Here, a large volume of relatively warm fresh meltwater would cover the dense, previously glacial, cold, and salty ocean. This plumeworld hypothesis was originally proposed to explain the globally preserved cap carbonates (Allen & Hoffman, 2005; Shields, 2005). Sulfur isotope measurements (Shen et al., 2008), as well as magnesium and strontium isotope measurements (Liu, Wang, Raub, Macdonald, & Evans, 2014) of the post-Marinoan cap dolostone, are all consistent with the idea that the carbonate precipitated in a globally stratified ocean. These ideas have been further bolstered by Ca^{2+} and Mg^{2+} isotope work (Ahm, Bjerrum, Blättler, Swart, & Higgins, 2018), which place additional constraints on the $\delta^{13}C$ of dissolved inorganic carbon. Estimates of the stratification timescale vary and have recently been extended to be as long as 50,000 years (with lower estimates at 8,000 years; Liu et al., 2014; Yang et al., 2017). Related to these estimates, the inferred deposition rates of cap carbonates are also uncertain, ranging from 10^2 years (Hoffman et al., 1998) up to 10^5 years (Font, Nédélec, Trindade, & Moreau, 2010; Higgins & Schrag, 2003; Trindade, Font, D'Agrella-Filho, Nogueira, & Riccomini, 2003).

Previous studies have addressed general carbon cycling in Neoproterozoic stratigraphic sections immediately postdating the Marinoan glaciation (Hoffman et al., 1998; Hoffman & Schrag, 2002; Sansjofre et al., 2011). These units characteristically capture evolving carbonate carbon isotope compositions, but (as noted above) are less commonly complemented by the carbon isotope composition of corresponding organic matter. When this has been done, for example, isotopic variability in the offset between carbonate and organic matter has been used to argue for low post-glacial CO_2 (Sansjofre et al., 2011)—this is in stark contrast to climate models (Hoffman et al., 2017; Pierrehumbert, 2010) and minor oxygen isotopes in Mainoan cap-barite crystal fans (Bao et al., 2008). Following on this work, in this study we present $\delta^{13}C$ data of carbonate and organic matter from two post-Marinoan sections that show particularly anomalous $\delta^{13}C_{org}$ signals—an isotopic character yet unseen in the Neoproterozoic.

2 | GEOLOGICAL SETTING

We focus on two well-studied post-Marinoan stratigraphic sections, the Ol Formation in Mongolia (Macdonald, Jones, & Schrag, 2009) and the Sheepbed Formation in the Yukon (Johnston et al., 2013; Macdonald et al., 2013). These two stratigraphic units cover similar periods of time (and are anchored on glacial deposits), but also carry important lithological differences that allow further interpretive insight. Overall, however, these sections provide a window into carbon cycling on platform margins during the immediate aftermath of the Marinoan snowball Earth. The geological setting and regional setting, along with basin interpretations, are provided elsewhere (Macdonald et al., 2009, 2013); however, we do provide a facies description and stratigraphic columns in Figure 1.

The Ol Formation sharply overlies glacial deposits of the Khongor Formation and is composed of ~7 m of dolostone succeeded by ~20 m of limestone. This cap dolostone consists of buff to pink-colored, largely recrystallized micropeloidal dolomite, while the overlying limestones start with buff limestone ribbonite (nodular bedded calcisiltite), succeeded by gray rhythmite (flat, graded beds of micrite and calcisiltite), iron-rich siltstone interbedded with marly carbonate, and gray grainstone (Macdonald et al., 2009). Above the cap dolomite, the carbonate rocks are mostly limestone, with the occasional presence of partially dolomitized carbonates (Bold et al., 2016). Sea floor cements made mainly of aragonite pseudomorphs are observed at the limestone–dolostone transition, present either as individual blades growing into overlying sediment or as crystal fan shrubs (Macdonald, 2011). The cap dolostone, ribbonite, and rhythmite are interpreted to represent a transgressive systems tract culminating with a maximum flooding surface in the iron-rich siltstone, and succeeded by a highstand systems tract in the overlying grainstone. Importantly, Neoproterozoic carbonate strata were deposited on an isolated carbonate platform margin and ramp (Bold et al., 2016), analogous to the modern Bahama Bank, and there is little evidence of terrestrial input throughout the succession.

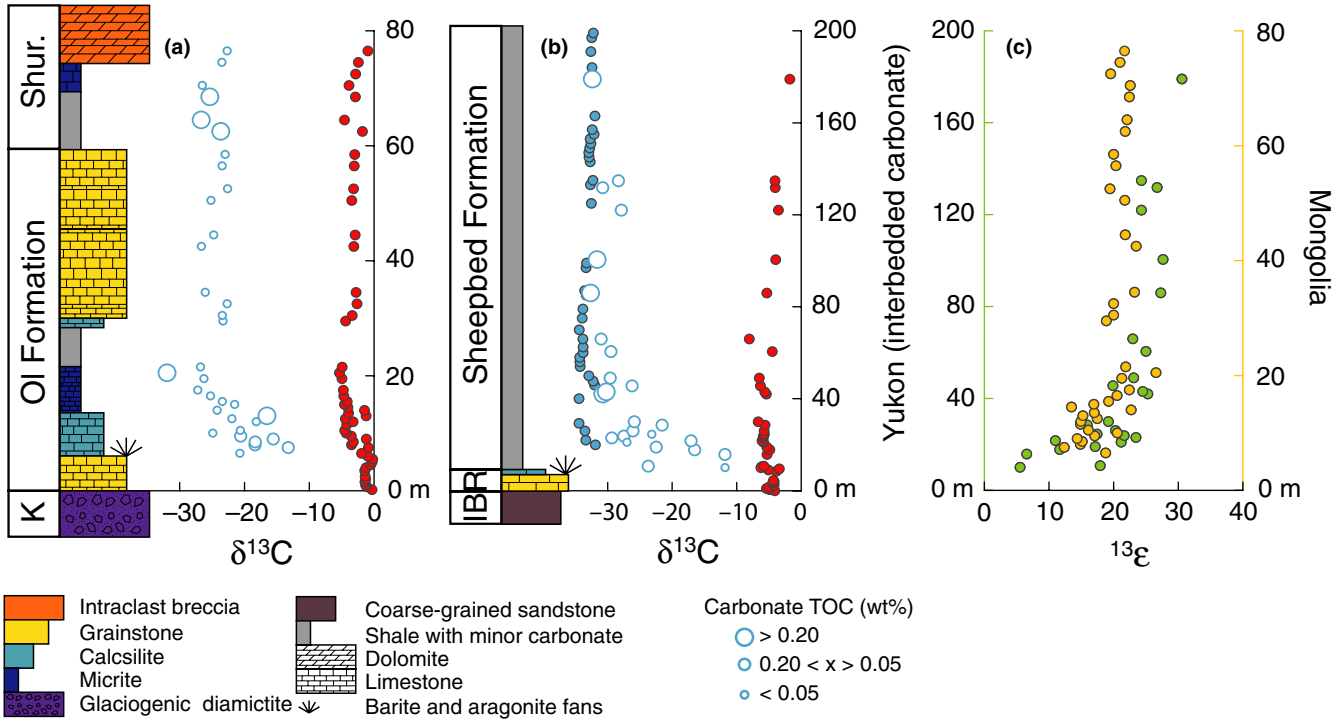

FIGURE 1 Presented are the sections containing anomalous $\delta^{13}C_{org}$ signals. The Mongolian Ol Formation is carbonate (a), whereas the Sheepbed Formation from the Yukon is predominantly siliciclastic with interbedded carbonates (b). Red circles are $\delta^{13}C_{carb}$ values. Open blue circles are the composition of organics from the carbonates ($\delta^{13}C_{org-c}$), while closed blue circles are the composition of bulk TOC from shale ($\delta^{13}C_{org-s}$). The $\varepsilon_{org-carb}$ for both sections are plotted together at right (c), with different *Y*-axis scales

The Sheepbed Formation overlies the ~1 m Hayhook limestone, the ~30-m-thick Ravensthroat cap dolostone and laterally discontinuous wedges of the Marinoan Stelfox diamictite. The thickness of the Sheepbed Formation varies between 200 and 600 m and is composed of shale with thin limestone interbeds. The shale from the lower 100 m of the Sheepbed is the most fissile and is likely to represent the maximum flooding surface of the post-Marinoan snowball recovery (Johnston et al., 2013; Macdonald et al., 2013). In the highstand systems tract of the upper Sheepbed Formation, siltstone and dolostone interbeds become more common before transitioning into dolomite of the Gametrail Formation.

3 | ANALYTICAL METHODS

Isotope data are presented using standard delta notation with units of permil (‰) reported relative to the Vienna PeeDee Belemnite (VPDB) standard. Measurements of $\delta^{13}C_{carb}$ and $\delta^{13}C_{org}$ were made separately, but where possible, are from the same hand sample. Carbonate samples were first cut and then micro-drilled on the exposed surface to obtain 5–20 mg of powder. Samples that showed visible secondary alteration, veining, fractures, and large siliciclastic components were avoided. Analyte CO_2 was collected cryogenically from the powdered samples by reaction in a common, purified H_3PO_4 bath at 90°C. The subsequent $\delta^{13}C_{carb}$ analyses were made with a VG Optima dual-inlet mass spectrometer attached to a VG Isocarb preparation device with a precision of ±0.2. Organic matter was extracted after decalcification in concentrated HCl for 48 hr. This residue was then analyzed with a Carlo Erba Elemental Analyzer attached to a ThermoFinnigan Delta V configured in continuous flow mode. External error of this measurement was ±0.3 for $\delta^{13}C$ and ±0.05 wt% for TOC. For the Sheepbed Formation, we measured both the $\delta^{13}C_{org}$ from the organic matter in carbonate lenses and the $\delta^{13}C_{org}$ from the organic matter in the shale. The Ol Formation had no significant siliciclastic beds, so the $\delta^{13}C_{org}$ measurements all come from carbonates.

4 | GEOCHEMICAL RESULTS

The $\delta^{13}C$ data of both carbonate and organic matter from our measured sections are presented in Figure 1. The Ol and Sheepbed formation carbonates are both isotopically light—a characteristic of post-snowball Earth deposits. The Sheepbed carbonate has an average value of −5.9 with a total range of 3.6. The Ol carbonate has an average value of −3.2 and carries a slight trend of increasing $\delta^{13}C_{carb}$ upsection, with a range of 4.5.

The Ol and Sheepbed formation $\delta^{13}C_{org}$, unlike the coeval $\delta^{13}C_{carb}$, have strongly variable compositions over these same intervals. Immediately after cap carbonate termination, the Ol Formation $\delta^{13}C_{org}$ carries a heavy composition of −13.3. Over the subsequent 10 m (moving upsection), the $\delta^{13}C_{org}$ decreases by ≈12, reaching a more characteristic $\delta^{13}C_{org}$ value of −25. In the subsequent 80 m, the $\delta^{13}C_{org}$ remains stable, with an average value of −24. In the Sheepbed

Formation, where we extracted and measured organic matter from both shale and interbedded carbonate lenses, only the carbonate-derived organic matter showed a similar anomaly to the OI Formation. The $\delta^{13}C_{org-c}$ (the $\delta^{13}C$ of organic matter sourced from the carbonate lenses) reaches its maximum value of −11.8 immediately above the cap carbonate, then over 20 m, the isotopic composition decreases before stabilizing at an average composition of −29.5. The $\delta^{13}C_{org-s}$ ($\delta^{13}C$ of organic matter sourced from the *s*hale) in contrast remains constant with a composition of −31 throughout the section.

The strongly variable $\delta^{13}C_{org}$ and near constant $\delta^{13}C_{carb}$ in both of these sections result in a correspondingly variable $\varepsilon_{org-carb}$ (the isotopic offset between phases). While the stratigraphic length scale over which this change occurs is different between the sections, both show a trend of initially sharply decreasing $\varepsilon_{org-carb}$ that subsequently stabilizes at more typical values (Hayes, Strauss, & Kaufman, 1999). The Sheepbed section approaches a $\varepsilon_{org-carb}$ of 24.5, while the OI approaches a $\varepsilon_{org-carb}$ of 21.5. Most notably, the $\varepsilon_{org-carb}$ of ≈8, as measured at the base of both sections, are extremely unusual in the geologic record.

Isotope data are accompanied by measurements of organic carbon content, noted as TOC. The TOC in both the OI and the Sheepbed are low, where only two samples from the OI exceeded 0.4%, and all of the Sheepbed samples are <0.3%. The OI sample with the greatest TOC is also an isotopic outlier, with a $\delta^{13}C_{org}$ 4.7 lighter than the next lightest sample. While all the samples have low TOC, the anomalous samples in the OI formation are relatively enriched in TOC compared to the overlying 40 m. This enrichment, however, is only barely resolvable given the 0.05% precision of the TOC measurement. The Sheepbed does not show the same trend, and the TOC of the isotopically anomalous samples, 0.06%, is not statistically different from the TOC of the section above.

The trend of increasing $\varepsilon_{org-carb}$ upsection in the Sheepbed and OI formations stands in contrast with typical post-cap carbonate sections where $\varepsilon_{org-carb}$ remains constant (see Figure S1). The light $\delta^{13}C_{carb}$ is characteristic of this time (Hoffman et al., 1998); however, the trend in $\delta^{13}C_{org}$ requires further explanation. Observing a similar $\delta^{13}C_{org}$ signal in two sections deposited in different paleo-basins and lithologies suggests that the process creating these signals may share an origin and may reflect some fundamental aspect of carbon cycling during the post-Marinoan world. However, the counterpart, wherein all other post-Marinoan sections do not carry this behavior, must also factor into any model describing these data (cf. Sansjofre et al. 2011).

5 | DISCUSSION

It is common for sedimentary organic matter to carry an isotopic composition offset from carbonate by roughly 20–30 (Hayes et al., 1999; Johnston, Macdonald, Gill, Hoffman, & Schrag, 2012). For the majority of the stratigraphy examined for this study, the $\varepsilon_{org-carb}$ is indeed within this window with a mean of 22.6 and in keeping with observations from sedimentary units younger than 800 million years old (Hayes et al., 1999). These more typical observations are contrasted with exceedingly small $\varepsilon_{org-carb}$ values lower in the OI and Sheepbed formations—these minimal isotopic offsets require additional or perhaps even atypical behavior within the marine carbon cycle. These observations can thus be considered in a variety of fashions, from interrogating the variability within fractionation factors themselves, to physical changes in the ocean–atmosphere system during deglaciation that might enable the production and preservation of the observed signal.

To enable this discussion and quantitatively consider the consequences of a post-glacial ocean, we developed a model that simulates the ocean–atmosphere system immediately after the termination of snowball Earth (Figure 2). This model updates and extends previous work on the hydrology and carbon geochemistry of the post-Marinoan recovery (Higgins & Schrag, 2003) and stands in complement to recent Ca^{2+} and Mg^{2+} isotope modeling (Ahm et al., 2018). The explicit goal is to quantitatively explain both the more common $\delta^{13}C$ values and the anomalous $\varepsilon_{org-carb}$. To do so, we track the flux and isotopic composition of carbon—as well as the flux of other biogeochemically significant elements like phosphorus and calcium—between three boxes: the atmosphere, surface ocean, and deep ocean. Organic matter and carbonate produced in the surface ocean box contribute to a modeled sedimentary record, which can be compared to the measured sections. Given modern inputs, the model is conservatively tuned to approach a steady state that reflects roughly modern conditions for atmospheric CO_2 concentration, f_{org}, dissolved inorganic carbon (DIC) partitioning, carbon export flux, and carbon isotope fractionation. Further, when modeling the post-glacial recovery, the model incorporates new thinking on marine stratification timescales (Yang et al., 2017). The initial parameterization of the model best reflects the conditions immediately after snowball Earth (Bao et al., 2008; Kasemann, Hawkesworth, Prave, Fallick, & Pearson, 2005; Sansjofre et al., 2011). A full model description and extensive sensitivity test are provided in Appendix S1.

The treatment presented herein is set to target the carbon isotope outputs of the ocean and atmosphere system. Importantly, recent work highlights the dynamics between surface and deep ocean exchange in the snowball aftermath (Yang et al., 2017). For instance, it has been suggested that the stratified post-snowball ocean could last for upwards 50,000 years before modern-like circulation resumes—meaning that the ocean could be strongly heterogeneous with respect to the isotopic composition of DIC. We track this feature, as mixing is initially set such that the deep ocean overturns with an e-folding time of 50,000 years, and then relaxes to a residence time of 2,000 years (Figure S3). It is also expected that in the immediate post-snowball Earth, high atmospheric CO_2 drives the surface ocean to low pH. On a longer time scale, the DIC, alkalinity, and pH of the surface ocean recover as a function of continental weathering inputs. The strong density stratification between the surface and deep ocean inhibits immediate thermohaline circulation and isolates the surface ocean. This means that very little of the surface ocean DIC increase originates from the deep ocean upwelling. Due to this gradual buildup of alkalinity, carbonate precipitation does not occur

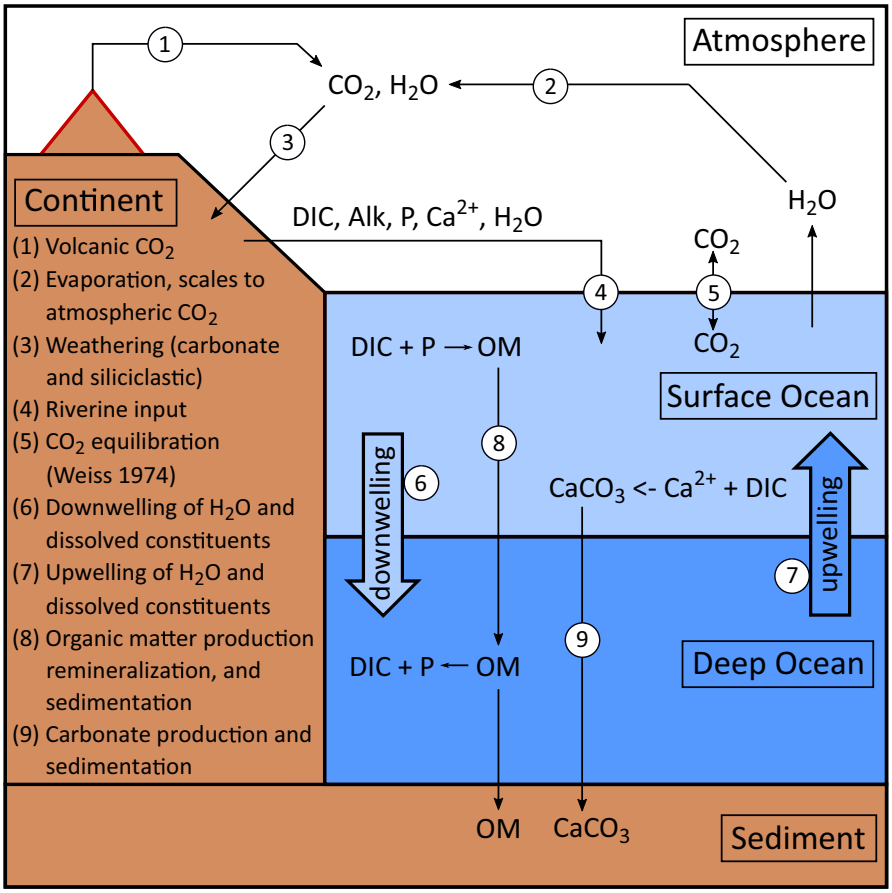

FIGURE 2 The boxes and fluxes of the carbon isotope model. The volcanic CO_2 flux is the only net source of carbon to the system (1), while organic matter and carbonate deposition are the only net sink (8–9). Water and all other species of interest—primarily carbon but also phosphate, salinity, and oxygen—are exchanged between the boxes through riverine weathering (3–4), gas exchange (5), hydrothermal circulation (6–7), and particle sinking (8–9)

immediately after deglaciation; instead, riverine fluxes must increase surface ocean [Ca^{2+}] and [CO_3^{2-}] sufficiently to reach supersaturation. This time gap is a feature not expressed in a well-mixed single box ocean model and may help explain the cap carbonates characteristically abrupt basal contact (Hoffman & Schrag, 2002). For most marine chemical signatures (salinity, DIC, pH, etc), the model illustrates heterogeneity between the surface and deep ocean, which quickly converge after the resumption of vigorous thermohaline circulation.

In interpreting carbon isotopes, it is important to recognize that both the oxidized (carbonate) and reduced (organic matter) components of the carbon cycle are represented in the geological record. As carbonate is interpreted as reflective of DIC, it is appropriate to begin with an analysis of sedimentary $\delta^{13}C_{carb}$. As captured in Figure 1, carbonate carbon initially carries a $\delta^{13}C$ of −2, before decreasing to a minimum of −5. With time, the isotopic composition of carbonate gradually increases. These same stratigraphic observations have been previously explained by varying features like the temperature at which the carbonate precipitates (Higgins & Schrag, 2003), and sediment-buffering/isotopic resetting (Ahm et al., 2018). However, temperature is a key component of our model and linked to atmospheric CO_2, and cannot be independently varied to satisfy carbonate $\delta^{13}C$. Instead, the composition of carbonate is accounted for via Rayleigh fractionation during the rapid draw down and subsequent precipitation of the large atmospheric CO_2 pool (Hoffman et al., 1998) and by decreasing f_{org}, a mechanism classically invoked to shift $\delta^{13}C_{carb}$ (Hayes et al., 1999). In addition to those listed above, we consider contributions from carbonate versus silicate weathering, the composition of weathered carbonates, changes in atmospheric CO_2 and volcanic out-gassing, and variable phosphate availability. A full sensitivity test of these parameters is available in Appendix S1.

After considering model implications for external perturbations to the marine carbon cycle, we are left looking at the inter-workings of the system itself, namely how organic carbon is generated and how it adopts its associated isotopic composition. The fractionation factor describing this process ($\varepsilon_{org-carb}$) can be roughly divided into two main components, the direct biological contribution of carbon fixation to $\varepsilon_{org-carb}$ and the inorganic carbon speciation that sets $\delta^{13}C_{DIC}$ (acknowledging the role of diagenesis in slightly altering $\varepsilon_{org-carb}$; Ahm et al., 2018; Oehlert & Swart, 2014). Quantitatively, fractionation factors respond most strongly to different environmental factors. The inorganic component of $\varepsilon_{org-carb}$ is driven by the temperature-dependent equilibrium fractionation between carbon species. For example, higher temperatures produce a smaller fractionation. Due to the elevated greenhouse gas concentration (as demonstrated in Figure S3), the surface ocean temperature where the carbonate precipitation occurs was greatest shortly after deglaciation and quickly decreases as pCO_2 is drawn down. This decrease in temperature, and corresponding increase in equilibrium fractionation, corresponds in directionality to what is preserved in the geologic record, but falls short of a silver bullet (Figure 3b). It has also been argued that the $\delta^{13}C$ of DIC and the resulting carbonates are

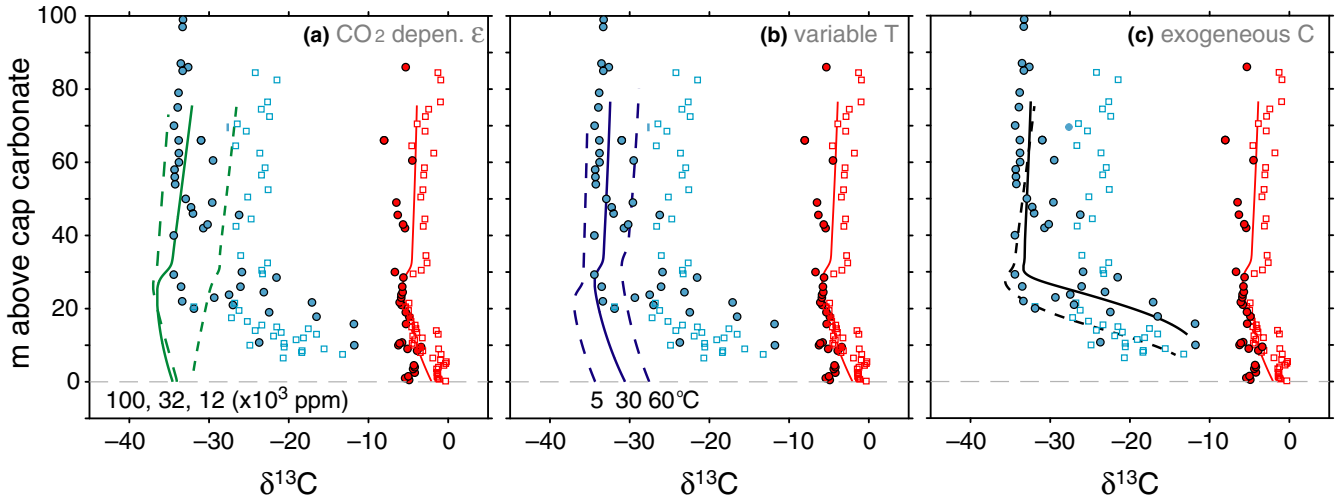

FIGURE 3 Comparisons between various model predictions and the measured data. Note that all model outputs carry significant detail, as outlined in the SOM, and lead to some non-linear behavior as it relates to the scaling of the variables in question. (a) When the ε_p is parameterized as a function of CO_2 concentration, it carries a large consequence for $\varepsilon_{org-carb}$. (b) Here, ε_p is fixed and surface ocean temperature is prescribed. Higher temperatures generate isotopically heavier $\delta^{13}C_{org}$ (c) The prediction based on anomalous carbon inputs (see text) for the middle scenarios in (a and b). The model behavior near the base of the stratigraphic sections reflects the post-glacial disequilibrium and how the system approaches carbonate saturation, surface ocean–atmospheric equilibrium, all of which are proportional to reservoir size

diagenetically altered along geochemical gradients associated with the vigor of pore water versus seawater exchange (Ahm et al., 2018; Higgins et al., 2018). One exciting and directly applicable result of that work is revised estimates of the $\delta^{13}C$ of DIC in the post-Marinoan surface ocean (Ahm et al., 2018). These estimates, which extend down to −11, only make understanding the $\delta^{13}C$ of organic matter in our measured sections more difficult to explain (when related to offsets from DIC).

The biological component of $\varepsilon_{org-carb}$, primarily ε_p, is also environmentally dependent. Much experimental work illustrates that this fractionation is dependent on CO_2 concentration, microbial growth rate, and surface-to-volume ratio of the organism or cell (Popp et al., 1998). We directly incorporate this CO_2 dependence (Figure 3a), where growth rate is set as a function of continental weathering, and surface-to-volume ratio is assumed constant. At elevated extracellular CO_2 concentrations, consistent with the post-Marinoan world, the ε_p becomes larger. Therefore at the beginning of the model simulation, when CO_2 concentrations are greatest, the ε_p value is correspondingly large. Large ε_p would tend to produce large $\varepsilon_{org-carb}$, an observation that is strongly incompatible with the presence of the $\delta^{13}C_{org}$ anomaly. One might also consider a local disequilibrium driven by rapid CO_2 drawdown by microbial mats. This could aid in changing the observed $\varepsilon_{org-carb}$ value (Hoffman, Macdonald, & Halverson, 2011; Lorian, Erez, & Lazar, 1992), but would have counter-acting effects on the $\delta^{13}C$ of local DIC (Ahm et al., 2018; Falk et al., 2016).

In more detail, environmental controls, and specifically ties to pCO_2, have counter-acting effects on the isotopic offset between carbonate and organic matter. High temperatures tend to decrease equilibrium isotope effects, while high dissolved CO_2 concentrations tend to increase ε_p. One might envision the physiological response as acting as a stronger lever; however, this would require an initial CO_2 concentration of 400 ppm followed by a gradual increase to 1,500 ppm to satisfy the observations. This contradicts both the geologic evidence of cap carbonates and the geochemical/climatological models of elevated CO_2. If we forgo the environmental dependence of ε_p and instead impose a single fractionation factor for primary production, temperature becomes the dominant variable controlling $\varepsilon_{org-carb}$. However, realistic temperature changes (for instance cooling the ocean from 30 to 5°C) only accommodate about 3 of the required 15 anomaly captured in the organic matter. This also suggests that extracting paleo-barometric data from these records is beyond the current calibration of the carbon isotope system (Sansjofre et al., 2011).

Through the analysis of model results, what is clear is that an atypical carbon cycle is required to explain the anomalous isotopic composition of organic matter. A full model sensitivity analysis, demonstrating the isotopic leverage of changes in stratification timescales, hydrologic cycling, weathering intensity and protolith, riverine and P fluxes, volcanism, carbonate precipitation dynamics, and many more (see Figures S4–S7), is captured in Appendix S1. In short, these affiliated geochemical changes cannot account for the $\delta^{13}C$ observations.

It has been previously suggested an additional organic matter flux (such as from weathering) could contribute to preserved marine records (Johnston et al., 2012). Given isotope mixing, this additional organic matter must have a reservoir size and prescribed isotopic composition. For example, in Figure 2, the model above produces an organic carbon flux with a composition of −35, but the bulk sedimentary $\delta^{13}C_{org}$ is about −12. This overall value can be produced either by mixing a small amount of very heavy organic carbon or a large amount of relatively lighter (though still very heavy) organic

matter. For instance, mixing in an anomalous composition of 20 would require a 42% contribution to the bulk sedimentary $\delta^{13}C_{org}$, whereas mixing in an anomalous composition of −10 would require a 92% contribution (recall that marine primary production is set by the geochemical component of the model). The only strict constraint is that the anomalous carbon must be heavier than the heaviest sedimentary $\delta^{13}C_{org}$ value of −11.8.

To fit the stratigraphic trend in the data (Figure 2c), we model this anomalous contribution following an exponential decay function as some still theoretical pool of carbon is gradually depleted in mass. The combined $\delta^{13}C_{org}$ (isotopically normal organic matter plus an exogeneous source) is described by the following function:

$$\frac{\delta^{13}C_{org-combined}}{dt} = \frac{J_{org}\cdot\delta_{org} + J_{anomalous}\cdot(e^{-k\cdot t})\cdot\delta_{anomalous}}{J_{org} + J_{anomalous}\cdot(e^{-k\cdot t})}, \quad (1)$$

where J_{org} is the flux of normal organic matter to the sediment, δ_{org} is the isotopic value of that normal organic matter, $J_{anomalous}$ is the initial flux of anomalous carbon, k is a decay constant tied to the anomalous flux, and $\delta_{anomalous}$ is the isotopic value of the anomalous carbon pool. This is simply a fitting exercise where calculating an anomalous contribution assumes that the magnitude of any anomalous flux is dependent only on the time elapsed and the initial flux. A linear mixing model could also be sufficient to explain the data, but given the nature of the upsection trend, we prefer an exponential relationship. Further, we imply no specific age model for these sections or the fit, but would imply that the fit suggests relatively constant sediment deposition in each locality. This assumption can be revisited if the source of the $\delta^{13}C_{org}$ anomaly is uniquely identified. To that point, the solution to this mixing problem is non-unique. Practically, however, it is still difficult to produce the heavy organic matter being contributed to the marine realm, so we conservatively adopted an anomalous composition of −10. Given this composition, the sedimentary record can be fit by varying the sedimentation rate of the whole sequence and the decay constant (k) of the anomalous flux (Figure 2). The source of this organic matter and what controls it delivery remains open.

6 | ENVIRONMENTAL SIGNIFICANCE

The simple fact that the anomalous $\delta^{13}C_{org}$ is preserved in both Mongolia and the Yukon, but not elsewhere in the world, differentiates this anomaly from other, carbonate hosted excursions. More typical carbonate–organic matter relationships are preserved in Arctic Alaska (see SOM), China (Cui et al., 2017; Jiang et al., 2010; McFadden et al., 2008; Shen et al., 2008; Wang et al., 2016), and Brazil (Sansjofre et al., 2011), and are all compiled in Appendix S1. Put differently, the $\delta^{13}C_{org}$ in Northwest Canada and Mongolia is an outlier to that seen elsewhere; however, it does speak to a marine carbon cycle vulnerable (at least on the local scale) to exogenous contributions (Johnston et al., 2012) or differential diagenesis (Ahm et al., 2018; Higgins et al., 2018). Further, the relationship between TOC and the isotopic offset between organic matter and DIC is indeed broadly consistent with other Neoproterozoic marine basins (Figure S2). The answer to the mechanism behind this signal may in fact be encoded in where we find (and do not find) the heavy $\delta^{13}C_{org}$ values. Importantly, we note the following:

1. these sections are not located in the same paleo-basin, and
2. the signal is even manifest in different host lithologies.

The cause of the anomaly must be common enough to have independently arisen in two locations without being so prolific that it becomes globally distributed. This still begs the question of why Mongolia and the Yukon are similar to one another, yet different from other sampled post-Marinoan margins.

The OI and Sheepbed formations, in addition to being lithologically different, may also capture different depositional timescales. The Sheepbed Fm. carbon anomaly is formed over 20 m of siliciclastic deposition, while the OI carbon anomaly is formed over only 10 m of largely carbonate-dominated strata. This either speaks to the relative depositional rates (and the same overall time for the compared stratigraphy), or heterogeneity between sites. As carbonate production should outpace normal siliciclastic deposition, the stratigraphic reach of the anomaly in both sections is further exacerbated. This temporal variation, in addition to the spatial heterogeneity, further discourages the idea that a single global process could produce the observed anomalies.

The available data also allow for interrogation of how much organic matter is present within a sample (or section) as it relates to the accompanying isotopic composition. In the OI Formation, samples with anomalous $\delta^{13}C_{org}$ have significantly greater TOC than samples from the immediately overlying strata. This observation could be explained by a low background organic matter flux that mixed with a larger anomalous flux, summing to more TOC and a heavy isotopic composition (see Equation 1). The relative standard deviation is large on the TOC measurements, but observing the degree to which TOC increases in the anomalous section, the anomalous $\delta^{13}C_{org}$ possibly accounts for more than 80% of the organic matter in this section. This large contribution of anomalous organic matter to the observed sedimentary $\delta^{13}C_{org}$ would suggest that the original composition of the anomalous organic matter did not deviate significantly from the observed value of −13. This framework helps explain the OI Formation; however, the Sheepbed Formation data do not lend itself to the same mixing analysis. Recall the differences in the $\delta^{13}C_{org}$ between the host siliciclastics and the carbonate lenses, where only carbonate lenses record a signal similar to the Old Formation.

7 | ENVISIONING THE CARBON CYCLE

A common mathematical way to vary the $\varepsilon_{carb-org}$ in geochemical models is to decouple the organic matter production from DIC and carbonate precipitation. If, for example, there was a large reservoir of dissolved organic carbon in the deep ocean, it may be possible that the carbonate sampled one source, while the organic matter

sampled another (Rothman et al., 2003). Although theoretically plausible, our model cannot accommodate the observation, even with the imposition of a large post-Marinoan DOC reservoir (see SOM). In fact, even if deep ocean DOC was residually heavy from some previous event, there is no physical justification for suddenly precipitating/depositing this pool at the time of the excursion, and only on certain margins. Finally, the excursion occurs during a period of marine stratification in which the deep ocean is less, not more, likely to influence surface ocean and sedimentary processes.

If it is not possible to decouple the organic matter production from carbonate precipitation would, it instead be possible to change the environmental conditions in order to vary $\varepsilon_{carb-org}$? Some microbial metabolisms can produce unusually heavy organic matter, but not nearly as heavy as is required to satisfy these observations (Van Der Meer, Schouten, Leeuw, & Ward, 2000). As discussed earlier, producing an $\varepsilon_{carb-org}$ less than 10 solely by changing environmental conditions would require either low and increasing CO_2 concentrations or unrealistically high temperatures. Smaller isotopic signals, however, may be explained by differences in environmental conditions (Popp et al., 1998) or differential diagenesis (Ahm et al., 2018). It is possible that, for instance, the OI Formation was deposited in warmer waters, satisfying the smaller $\varepsilon_{carb-org}$ in the OI than the Sheepbed (21.5 vs. 24.5), but not the extremely small $\varepsilon_{carb-org}$ at the base of both sections. Ultimately, the most parsimonious model results match the sedimentary record more closely when ε_p is held constant, suggesting that either CO_2 was actually invariant over this time period, not likely, or that ε_p was not strongly dependent on CO_2.

Still in search of an explanation for generating such isotopically heavy organic matter, we can consider the idea that this organic material is either (a) heavily altered, (b) not marine in origin, (c) not contemporaneous with the sediments, or (d) some combination of all. In situ alteration at high-temperature can be ruled out given the relatively low grade of these units (see Appendix S1 for discussion). Isotopically heavy organic matter with $\delta^{13}C_{org}$ values comparable to the observed post-Marinoan anomaly can be found in modern hypersaline microbial mats (Schidlowski, Matzigkeit, & Krumbein, 1984). The evaporative environments increase nutrient concentrations and microbial growth rates until CO_2 becomes limiting, thereby reducing ε_p. Our model includes a parameter of increased evaporation due to the increased temperature and rapid hydrologic cycling, but the surface ocean salinity is also greatly reduced by stratification and glacial runoff during post-glacial time. Additionally, there is no geologic evidence of evaporite formation or extensive microbialites in the measured sections. Even without the specific hypersaline conditions, a sufficiently thick microbial mat may inhibit CO_2 diffusion and produce small ε_p values, but if this process was common we would expect to observe such small fractionation over the 3 billion-year history of microbial mat formation.

Anoxic conditions caused by prolonged stratification would have promoted the remineralization of sedimentary organic matter by methanogenesis, with a possible isotopic consequence for the residual organic carbon. Methanogenesis does produce methane depleted in ^{13}C, but porewater DIC, not the residual organic matter, adopts a complementary enriched ^{13}C composition (Conrad, Claus, & Casper, 2009; Whiticar, 1999). Producing the anomalous organic matter via methanogenesis would require the subsequent fixing of this DIC in sediment (Schrag, Higgins, Macdonald, & Johnston, 2013). Even if such a process occurred, it would not occur in sufficient magnitude necessary to produce the observed anomalies.

The most parsimonious explanation for these anomalies is still the addition of some unknown, exogenous, anomalous organic carbon flux to the background organic carbon deposition. This is taken from the clear, exponential decay of the signal upsection—a characteristic feature of diminished mixing of adjacent, isotopically distinct pools. However, our model does not assign a specific origin to this flux; instead, it provides a generic pool of heavy organic carbon that mixes with the background production. As noted earlier, the magnitude of this hypothetical flux is dependent on its isotopic composition. Simply reproducing the organic matter anomaly does not necessarily require the ultimate source of this anomalous OC be identified. Instead, as in Johnston et al. (2012), we may provide a general solution that is applicable regardless of the source of the anomaly, noting that the real challenge remains outstanding—how to generate such enriched organic matter.

One possible source of the anomalous organic carbon is the newly exposed continents. Glacial scouring during the snowball Earth event may have newly exposed an organic matter source that was subsequently imported to these marine basins by physical weathering (Hood et al., 2009). The anomalous carbon weathering from the continent also explains the two different $\delta^{13}C_{org}$ values in the Sheepbed section. The $\delta^{13}C_{org-s}$ values, consistently offset from $\delta^{13}C_{carb}$, probably sample organic matter produced contemporaneously in the photic zone. The $\delta^{13}C_{org-c}$, which carries the carbon isotope anomaly in the carbonate lenses, may have formed during pulsed weathering events. It is also critical to note the differing alteration histories of these two lithologies. In particular is the acknowledgment that the carbonate was surely subject to open system diagenesis, as evidenced by $\delta^{18}C_{carb}$ value (Macdonald et al., 2013) and arguments derived from heavier isotope systems (Ahm et al., 2018). Whatever the case, this decoupling disappears quite rapidly. Returning to the source of the organics, excess riverine input would deliver alkalinity to the DIC-rich surface ocean forming the carbonate lenses while simultaneously delivering the heavy organic matter weathered from the continent. Another possible transient source of organic matter to the sediment is from organic matter in cryoconite pans (Hoffman, 2016). This organic matter, closely associated with the glacier, would be released into the ocean as the ice receded. This organic matter would probably form in close equilibrium with atmospheric CO_2 and would therefore have typical light $\delta^{13}C_{org}$ values, not the −10 characteristic of the anomaly. However, isotopic arguments could indeed be met if the terrestrial source of the organic matter was weathering of higher metamorphic grade rocks in the hinterlands. It is understood that at higher temperatures, iron-bearing carbonate rocks can disproportionate (French, 1971), and in the process generate reduced carbon (cf. graphite) with a characteristic isotopic

composition similar to what is observed in both anomalous stratigraphic sections (>10; Chacko, Mayeda, Clayton, & Goldsmith, 1991, Van Zuilen, Lepland, & Arrhenius, 2002]. Challenging this interpretation, the OI formation has no geologic evidence of significant terrestrial input, nor is an obvious source rock located in the hinterlands.

8 | CONCLUSION

We present a coupled carbonate-organic matter record through post-Marinoan sedimentary successions in the Northwest Territories of Canada and Mongolia. The $\delta^{13}C$ of carbonate is characteristic of global trends, whereas the isotopic composition of the organic matter diverges from this global prediction. After a thorough tour of potential mechanisms that could drive such an effect, we are left without a unique environmental solution. The long-term stable stratification of the ocean in the immediate aftermath of the Neoproterozoic snowball Earth events is possibly unique in geologic history, but this environmental condition would not necessarily generate the anomalous $\delta^{13}C_{org}$ observed in the OI and Sheepbed formations. Prior explanations of anomalous $\delta^{13}C_{org}$ signals relied on the presence of a large deep ocean pool of DOC, but our model shows that even if such a pool existed, the stable stratification would make such a pool inaccessible to surface ocean processes (Rothman et al., 2003). Further these isotope signals do not reflect the effect of changing pCO_2 on algal physiology. Instead, the heavy $\delta^{13}C_{org}$ data can only sensibly be described by the addition of an exogenous, anomalous organic carbon flux to the sediment (Johnston et al., 2012), perhaps represented by higher temperature carbon reactions and subsequent weathering. We lack a unique solution for the generation of this organic matter; however, a non-marine solution would avoid the constraint imposed by buffering with a marine DIC budget. In the end, we are left with a robust, but challenging observation at an anomalous, but alluring period in Earth history.

ACKNOWLEDGMENTS

The authors would like to thank A. Pearson and the Johnston group for comments on early versions of this manuscript, as well as 2 anomalous reviewers for detailed comments that made the paper much stronger.

ORCID

Frasier L. Liljestrand https://orcid.org/0000-0002-1548-0487
Thomas A. Laakso https://orcid.org/0000-0002-2755-8050
David T. Johnston https://orcid.org/0000-0002-2487-1084

REFERENCES

Ahm, A.-S.-C., Bjerrum, C. J., Blättler, C. L., Swart, P. K., & Higgins, J. A. (2018). Quantifying early marine diagenesis in shallow-water carbonate sediments. *Geochimica et Cosmochimica Acta*, *236*, 140–159.

Allen, P. A., & Hoffman, P. F. (2005). Extreme winds and waves in the aftermath of a neoproterozoic glaciation. *Nature*, *433*(7022), 123–127.

Bao, H., Lyons, J., & Zhou, C. (2008). Triple oxygen isotope evidence for elevated CO_2 levels after a neoproterozoic glaciation. *Nature*, *453*(7194), 504–506.

Bold, U., Smith, E. F., Rooney, A. D., Bowring, S. A., Buchwaldt, R., Dudás, F. Ö., … Macdonald, F. A. (2016). Neoproterozoic stratigraphy of the Zavkhan terrane of Mongolia: The backbone for Cryogenian and early Ediacaran chemostratigraphic records. *American Journal of Science*, *316*(1), 1–63.

Chacko, T., Mayeda, T. K., Clayton, R. N., & Goldsmith, J. R. (1991). Oxygen and carbon isotope fractionations between CO_2 and calcite. *Geochimica et Cosmochimica Acta*, *55*(10), 2867–2882.

Cohen, P. A., Strauss, J. V., Rooney, A. D., Sharma, M., & Tosca, N. (2017). Controlled hydroxyapatite biomineralization in an 810 million-year-old unicellular eukaryote. *Science Advances*, *3*(6), e1700095.

Conrad, R., Claus, P., & Casper, P. (2009). Characterization of stable isotope fractionation during methane production in the sediment of a eutrophic lake, Lake Dagow, Germany. *Limnology and Oceanography*, *54*(2), 457–471.

Cox, G. M., Halverson, G. P., Stevenson, R. K., Vokaty, M., Poirier, A., Kunzmann, M., … Macdonald, F. A. (2016). Continental flood basalt weathering as a trigger for Neoproterozoic Snowball Earth. *Earth and Planetary Science Letters*, *446*, 89–99.

Cui, H., Kaufman, A. J., Xiao, S., Zhou, C., & Liu, X.-M. (2017). Was the Ediacaran Shuram Excursion a globally synchronized early diagenetic event? insights from methane-derived authigenic carbonates in the uppermost Doushantuo Formation, South China. *Chemical Geology*, *450*, 59–80.

Erwin, D. H., Laflamme, M., Tweedt, S. M., Sperling, E. A., Pisani, D., & Peterson, K. J. (2011). The Cambrian conundrum: Early divergence and later ecological success in the early history of animals. *Science*, *334*(6059), 1091–1097.

Falk, E., Guo, W., Paukert, A., Matter, J., Mervine, E., & Kelemen, P. (2016). Controls on the stable isotope compositions of travertine from hyperalkaline springs in Oman: Insights from clumped isotope measurements. *Geochimica et Cosmochimica Acta*, *192*, 1–28.

Font, E., Nédélec, A., Trindade, R., & Moreau, C. (2010). Fast or slow melting of the Marinoan snowball Earth? The cap dolostone record. *Palaeogeography, Palaeoclimatology, Palaeoecology*, *295*(1), 215–225.

French, B. M. (1971). Stability relations of siderite (FeCO3) in the system Fe-CO. *American Journal of Science*, *271*(1), 37–78.

Halverson, G. P., Hoffman, P. F., Schrag, D. P., Maloof, A. C., & Rice, A. H. N. (2005). Toward a Neoproterozoic composite carbon-isotope record. *Geological Society of America Bulletin*, *117*(9–10), 1181–1207.

Hayes, J. M., Strauss, H., & Kaufman, A. J. (1999). The abundance of 13c in marine organic matter and isotopic fractionation in the global biogeochemical cycle of carbon during the past 800 ma. *Chemical Geology*, *161*(1), 103–125.

Higgins, J. A., Blättler, C. L., Lundstrom, E. A., Santiago-Ramos, D. P., Akhtar, A. A., Crüger Ahm, A. S., … Swart, P. K. (2018). Mineralogy, early marine diagenesis, and the chemistry of shallow-water carbonate sediments. *Geochimica et Cosmochimica Acta*, *220*, 512–534.

Higgins, J. A., & Schrag, D. P. (2003). Aftermath of a snowball earth. *Geochemistry, Geophysics, Geosystems*, *4*(3). https://doi.org/10.1029/2002GC000403

Hoffman, P. (2016). Cryoconite pans on snowball earth: Supraglacial oases for cryogenian eukaryotes? *Geobiology*, *14*(6), 531–542. https://doi.org/10.1111/gbi.12191

Hoffman, P. F., Abbot, D. S., Ashkenazy, Y., Benn, D. I., Brocks, J. J., Cohen, P. A., … Warren, S. G. (2017). Snowball earth climate dynamics and Cryogenian geology-geobiology. *Science Advances*, *3*(11), e1600983.

Hoffman, P. F., Kaufman, A. J., Halverson, G. P., & Schrag, D. P. (1998). A neoproterozoic snowball earth. *Science*, *281*(5381), 1342–1346.

Hoffman, P. F., Macdonald, F. A., & Halverson, G. P. (2011). Chemical sediments associated with Neoproterozoic glaciation: Iron formation, cap carbonate, barite and phosphorite. *Geological Society, London, Memoirs*, *36*(1), 67–80.

Hoffman, P. F., & Schrag, D. P. (2002). The snowball earth hypothesis: Testing the limits of global change. *Terra Nova*, *14*(3), 129–155.

Hood, E., Fellman, J., Spencer, R. G., Hernes, P. J., Edwards, R., D'Amore, D. & Scott, D. (2009). Glaciers as a source of ancient and labile organic matter to the marine environment. *Nature*, *462*(7276), 1044.

Hurtgen, M. T., Arthur, M. A., Suits, N. S., & Kaufman, A. J. (2002). The sulfur isotopic composition of neoproterozoic seawater sulfate: Implications for a snowball earth? *Earth and Planetary Science Letters*, *203*(1), 413–429. https://doi.org/10.1016/S0012-821X(02)00804-X

Jiang, G., Wang, X., Shi, X., Zhang, S., Xiao, S., & Dong, J. (2010). Organic carbon isotope constraints on the dissolved organic carbon (DOC) reservoir at the Cryogenian–Ediacaran transition. *Earth and Planetary Science Letters*, *299*(1–2), 159–168.

Johnston, D. T., Macdonald, F. A., Gill, B., Hoffman, P., & Schrag, D. P. (2012). Uncovering the Neoproterozoic carbon cycle. *Nature*, *483*(7389), 320–323.

Johnston, D., Poulton, S., Tosca, N., O'brien, T., Halverson, G., Schrag, D., & Macdonald, F. (2013). Searching for an oxygenation event in the fossiliferous Ediacaran of northwestern Canada. *Chemical Geology*, *362*, 273–286.

Kasemann, S. A., Hawkesworth, C. J., Prave, A. R., Fallick, A. E., & Pearson, P. N. (2005). Boron and calcium isotope composition in Neoproterozoic carbonate rocks from Namibia: Evidence for extreme environmental change. *Earth and Planetary Science Letters*, *231*(1), 73–86.

Knoll, A. H. (2003). Biomineralization and evolutionary history. *Reviews in Mineralogy and Geochemistry*, *54*(1), 329–356.

Li, Z.-X., Bogdanova, S. V., Collins, A. S., Davidson, A., De Waele, B., Ernst, R. E., … Vernikovsky, V. (2008). Assembly, configuration, and break-up history of Rodinia: A synthesis. *Precambrian Research*, *160*(1), 179–210.

Liu, C., Wang, Z., Raub, T. D., Macdonald, F. A., & Evans, D. A. (2014). Neoproterozoic cap-dolostone deposition in stratified glacial meltwater plume. *Earth and Planetary Science Letters*, *404*, 22–32.

Lorian, D., Erez, J., & Lazar, B. (1992). Stable carbon isotopes in the reef ecosystem of the Gulf of Eilat—Red Sea. In *Proceedings of 7th international coral reef symposium* (Vol. *364*, pp. 243–247). Mangilao, Guam: University of Guam.

Macdonald, F. A. (2011). The Tsagaan Oloom Formation, southwestern Mongolia. *Geological Society, London, Memoirs*, *36*(1), 331–337.

Macdonald, F. A., Jones, D. S., & Schrag, D. P. (2009). Stratigraphic and tectonic implications of a newly discovered glacial diamictite–cap carbonate couplet in southwestern Mongolia. *Geology*, *37*(2), 123–126.

Macdonald, F. A., Strauss, J. V., Sperling, E. A., Halverson, G. P., Narbonne, G. M., Johnston, D. T., … Higgins, J. A. (2013). The stratigraphic relationship between the Shuram carbon isotope excursion, the oxygenation of Neoproterozoic oceans, and the first appearance of the Ediacara biota and bilaterian trace fossils in northwestern Canada. *Chemical Geology*, *362*, 250–272.

McFadden, K. A., Huang, J., Chu, X., Jiang, G., Kaufman, A. J., Zhou, C., … Xiao, S. (2008). Pulsed oxidation and biological evolution in the Ediacaran Doushantuo Formation. *Proceedings of the National Academy of Sciences*, *105*(9), 3197–3202.

Oehlert, A. M., & Swart, P. K. (2014). Interpreting carbonate and organic carbon isotope covariance in the sedimentary record. *Nature Communications*, *5*, 4672.

Pierrehumbert, R. T. (2010). *Principles of planetary climate*. Cambridge University Press.

Popp, B. N., Laws, E. A., Bidigare, R. R., Dore, J. E., Hanson, K. L., & Wakeham, S. G. (1998). Effect of phytoplankton cell geometry on carbon isotopic fractionation. *Geochimica et Cosmochimica Acta*, *62*(1), 69–77.

Rothman, D. H., Hayes, J. M., & Summons, R. E. (2003). Dynamics of the Neoproterozoic carbon cycle. *Proceedings of the National Academy of Sciences*, *100*(14), 8124–8129.

Sansjofre, P., Ader, M., Trindade, R., Elie, M., Lyons, J., Cartigny, P., & Nogueira, A. (2011). A carbon isotope challenge to the snowball earth. *Nature*, *478*(7367), 93–96.

Schidlowski, M., Matzigkeit, U., & Krumbein, W. E. (1984). Superheavy organic carbon from hypersaline microbial mats. *Naturwissenschaften*, *71*(6), 303–308.

Schrag, D. P., Higgins, J. A., Macdonald, F. A., & Johnston, D. T. (2013). Authigenic carbonate and the history of the global carbon cycle. *Science*, *339*(6119), 540–543.

Shen, B., Xiao, S., Kaufman, A. J., Bao, H., Zhou, C., & Wang, H. (2008). Stratification and mixing of a post-glacial Neoproterozoic ocean: Evidence from carbon and sulfur isotopes in a cap dolostone from northwest China. *Earth and Planetary Science Letters*, *265*(1), 209–228.

Shields, G. A. (2005). Neoproterozoic cap carbonates: A critical appraisal of existing models and the plumeworld hypothesis. *Terra Nova*, *17*(4), 299–310.

Swanson-Hysell, N. L., Rose, C. V., Calmet, C. C., Halverson, G. P., Hurtgen, M. T., & Maloof, A. C. (2010). Cryogenian glaciation and the onset of carbon-isotope decoupling. *Science*, *328*(5978), 608–611.

Trindade, R., Font, E., D'Agrella-Filho, M., Nogueira, A., & Riccomini, C. (2003). Low-latitude and multiple geomagnetic reversals in the Neoproterozoic Puga cap carbonate, Amazon craton. *Terra Nova*, *15*(6), 441–446.

Van Der Meer, M. T., Schouten, S., De Leeuw, J. W., & Ward, D. M. (2000). Autotrophy of green non-sulphur bacteria in hot spring microbial mats: Biological explanations for isotopically heavy organic carbon in the geological record. *Environmental Microbiology*, *2*(4), 428–435.

Van Zuilen, M. A., Lepland, A., & Arrhenius, G. (2002). Reassessing the evidence for the earliest traces of life. *Nature*, *418*(6898), 627.

Wang, X., Jiang, G., Shi, X., & Xiao, S. (2016). Paired carbonate and organic carbon isotope variations of the Ediacaran Doushantuo Formation from an upper slope section at Siduping, South China. *Precambrian Research*, *273*, 53–66.

Whiticar, M. J. (1999). Carbon and hydrogen isotope systematics of bacterial formation and oxidation of methane. *Chemical Geology*, *161*(1–3), 291–314.

Yang, J., Jansen, M. F., Macdonald, F. A., & Abbot, D. S. (2017). Persistence of a freshwater surface ocean after a snowball earth. *Geology*, G38920–G38921. https://doi.org/10.1130/G38920.1

SUPPORTING INFORMATION

Additional supporting information may be found online in the Supporting Information section.

How to cite this article: Liljestrand FL, Laakso TA, Macdonald FA, Schrag DP, Johnston DT. Isotopically anomalous organic carbon in the aftermath of the Marinoan snowball Earth. *Geobiology*. 2020;18:476–485. https://doi.org/10.1111/gbi.12383